

CASE FILE
COPY

NACA TN 3913

NATIONAL ADVISORY COMMITTEE
FOR AERONAUTICS

TECHNICAL NOTE 3913

SUMMARY OF 65-SERIES COMPRESSOR-BLADE LOW-SPEED CASCADE
DATA BY USE OF THE CARPET-PLOTTING TECHNIQUE

By A. Richard Felix

Langley Aeronautical Laboratory
Langley Field, Va.



Washington
February 1957

NATIONAL ADVISORY COMMITTEE FOR AERONAUTICS

TECHNICAL NOTE 3913

SUMMARY OF 65-SERIES COMPRESSOR-BLADE LOW-SPEED CASCADE

DATA BY USE OF THE CARPET-PLOTTING TECHNIQUE¹

By A. Richard Felix

SUMMARY

The carpet-plotting technique is presented herein as a more useful and concise method of summarizing the NACA 65-series compressor-blade cascade data given in NACA Technical Note 3916. Four different carpet plots are presented. Two of these plots facilitate the selection of blade camber and design angle of attack required to fulfill a design vector diagram. Since off-design compressor considerations are often as important as those of design, the third carpet plot facilitates the prediction of off-design turning angles at constant blade settings, despite the fact that the cascade tests were made at constant inlet-air angles with the blade settings varied. The fourth carpet plot presents an isentropic pressure-rise coefficient as a function of inlet-air angle, turning angle, and entering Mach number to permit a rapid estimation of blade loading for various velocity diagrams.

INTRODUCTION

The low-speed cascade data for the NACA 65-series compressor blades reported in reference 1 have been used rather extensively in the design of single-stage and multistage axial-flow compressors. The selection of the blade section and the blade setting required to fulfill a velocity diagram at design conditions requires several interpolations and cross plots of the data presented in reference 1. In order to facilitate these interpolations, the data were plotted in the present paper by the use of a technique called carpet plotting, which is described in reference 2. This technique makes possible the presentation of a function of several independent variables on a single two-dimensional graph and hence lends itself very well to interpolations for intermediate values of the several variables. The data of reference 1, which are carpet plotted herein, represent a range of solidity σ from 0.5 to 1.5, inlet-air angle β_1 from 30° to 70° , and camber C_{l_0} from 0 to 2.4.

¹Supersedes recently declassified NACA Research Memorandum L54H18a by A. Richard Felix, 1954.

SYMBOLS

α	angle of attack
C_{l_0}	blade camber (isolated airfoil lift coefficient)
σ	blade solidity
β	inlet-air angle
θ	turning angle
R	substitute value replacing θ in carpet plots, $\theta + 50(C_{l_0} - 0.4)$ (see appendix)
ΔP	static pressure rise across blading
q	dynamic pressure
M	Mach number
Subscripts:	
d	design value
1	upstream of blading

CARPET PLOTS

Since the carpet-plotting technique is not too well known, a description of this technique is included in the appendix. The feature which provides the utility of a carpet plot and differentiates it from other plots is the use of an abscissa scale with a shifting origin. The origin is shifted in the x-direction a distance proportional to the increment of the variable being represented. All figures herein have been reproduced large size and are placed in the envelope attached to the back cover.

The usual procedure in blade-section selection is to determine the camber C_{l_0} , which is required for a given design velocity diagram at a selected solidity. Figure 1 gives carpet plots of the data of reference 1 at five solidity conditions. The carpet plots indicate the variation of camber C_{l_0} at design angle of attack α_d with required values of inlet-air angle β_1 and design turning angle θ_d . Each carpet plot is spaced from the next by a number of grid units proportional

to the difference in solidities. In reference 1, it was established that the design angle of attack is independent of inlet-air angle. It is therefore possible to present a carpet plot (fig. 2) showing design angle of attack α_d as a function of camber C_{l_0} and solidity σ .

The tests in reference 1 were made at fixed inlet-air angles with the angle-of-attack variation produced by changing the blade setting. Although data of this type facilitated the determination of design conditions for the various combinations of inlet-air angle, solidity, and camber, it does not lend itself easily, as presented, to obtaining off-design performance of a blade section as this section would operate in a compressor in which blade setting is fixed and the angle of attack varied by changing the inlet-air angle. However, if the data are plotted as an off-design carpet, it is a simple matter to draw in curves of constant blade setting and thus to predict the variation in turning angle with angle of attack for all intermediate conditions of solidity, camber, and blade setting. Such off-design carpet plots are presented (fig. 3) showing turning angle as a function of solidity, inlet-air angle, angle of attack, and camber. Off-design data are presented for the following sections:

NACA 65-(4A₁₀)10

NACA 65-(8A₁₀)10

NACA 65-(12A₁₀)10

NACA 65-(15A₁₀)10

NACA 65-(18A₁₀)10

It should be pointed out that the blade designations used in reference 1 are changed herein to conform with the system adopted in reference 3.

Pressure rise as a percentage of inlet dynamic pressure $\Delta P/q_1$, called pressure-rise coefficient, has been used as a cascade loading-limit parameter. It is known that cascade losses increase rapidly above certain limiting values of $\Delta P/q_1$. However, in view of the physical meaning of the pressure-rise coefficient, particularly in reference to the inner and outer casings, it is considered to be a useful parameter. If the inlet-air angle, the turning angle, and the entering Mach number are known, it is possible to calculate an isentropic pressure-rise coefficient provided some relationship is assumed between the entering and leaving stream-tube areas. Therefore, two carpet plots were made in order to show the variation of the pressure-rise coefficient with inlet-air angle β_1 , turning angle θ , and entering Mach number M_1 . The first of these plots (fig. 4(a)) was calculated by assuming constant stream-tube area;

the second (fig. 4(b)) was calculated by assuming that the stream-tube area varied so that constant axial velocity would be produced across the blade passage. Pressure-rise coefficients obtained from these two plots quite often bracket the value associated with the actual three-dimensional condition being examined.

SAMPLE OF USE OF CARPET PLOTS

The use of the carpet plots presented can be shown best by use of an example. Generally, from a velocity-diagram calculation, the inlet-air angle, turning angle, and inlet Mach number are known and some value of solidity has been decided upon. The problem is to find the camber C_{l_0} , the design angle of attack α_d , the pressure rise coefficient $\Delta P/q_1$ (one-dimensional flow being assumed), and the off-design variation in θ with α at a constant blade setting. The following design conditions are assumed:

$$\begin{aligned}\beta_1 &= 55^\circ \\ \theta_d &= 15^\circ \\ \sigma &= 1.10 \\ M_1 &= 0.65\end{aligned}$$

Figure 1 is used to locate first the intersection of the $\beta_1 = 55^\circ$ and $\theta_d = 15^\circ$ curves on each of the four carpets representing solidities of 1.25, 1.00, 0.75, and 0.50; then a smooth curve is drawn connecting these four points which will be called A, B, C, and D. If the β_1 and θ values had fallen between those represented on the curves, these intermediate values could be located by measuring the increments along the abscissa. Although the design solidity of 1.10 falls between points A and B representing solidities of 1.25 and 1.00, respectively, points C and D for solidities of 0.75 and 0.50 are included to define more accurately the shape of the curve between points A and B. Since the horizontal interval from A to B represents a solidity increment of 0.25 from 1.25 to 1.00, the point corresponding to a solidity of 1.10 may be obtained by locating on the ABCD curve the point E which has a horizontal distance from point B equal to a solidity increment of 0.10. Point E thus located indicates a camber of 0.87 on the ordinate scale.

Next, the solidity of 1.10 and the newly found camber of 0.87 are used in conjunction with figure 2 to find the design angle of attack. The point for a camber of 0.87 is located on the $\sigma = 1.10$ curve between the camber of 0.8 and 0.9 curves by reading the proper horizontal increment of 0.07. This point indicates on the ordinate scale a design angle of attack of 10.5° .

The pressure-rise coefficient $\Delta P/q_1$ is found from figure 4(a) by using the values $M_1 = 0.65$, $\beta_1 = 55^\circ$, and $\theta = 15^\circ$. In figure 4(a), the $\Delta P/q_1$ was calculated on a one-dimensional basis, whereas in figure 4(b) the $\Delta P/q_1$ was calculated for a constant axial velocity. Since one-dimensional flow was assumed in this example, figure 4(a) should be used. Employing the proper horizontal β_1 increment of 10° and starting at the $\beta_1 = 45^\circ$ curve, locate the $\beta_1 = 55^\circ$ point on the $\theta = 15^\circ$ curve for each of the carpet plots representing Mach numbers of 0.50, 0.60, 0.70, and 0.80. The four points thus located are designated F, G, H, and I and are connected by a smooth curve. Next, locate on this curve point J whose horizontal distance from point G is equal to a Mach number increment of 0.05. Point J indicates on the ordinate scale a pressure-rise coefficient of 0.590.

The last step in this sample problem is the prediction of an α, θ curve at a constant blade setting. The off-design carpet (fig. 3(f)) is used to predict this α, θ curve for the blade section having a camber of 0.87, a solidity of 1.10 and a blade setting of 44.5° . The blade setting is the difference between the inlet-air angle and the angle of attack, or $55^\circ - 10.5 = 44.5^\circ$ at the design condition. In figure 3(f), curves marked "a" and "b", representing this constant blade setting of 44.5° , are drawn on the θ, α, β_1 plots for the camber of 0.4 at the solidities of 1.25 and 1.00, respectively. Curve "c" is then interpolated for the solidity of 1.10 by the use of the correct solidity increment along the abscissa. As can be seen in the example, this interpolation is aided by drawing between curves "a" and "b" lines of constant angle of attack at values of $6^\circ, 8^\circ, 10^\circ, 12^\circ$, and 14° . A similar interpolation is then accomplished for a camber of 1.2, which produces curves "d," "e," and "f." A linear interpolation for the intermediate camber of 0.87 is made between curves "c" and "f" to obtain curve "g," which shows the variation of R with α for the design camber and solidity. The R values may be converted to θ values by using the relationship

$$\theta = R - 50(C_{l_0} - 0.4)$$

It has been found that linear interpolations between any two cambers of figure 3(f) produce design turning angles which agree with the design carpet plot within 1.0° . If greater accuracy is desired, a faired curve between the three cambers should be used. In this figure 3(f), the design angle of attack is indicated by a short-dashed line and the approximate occurrence of twice minimum drag is indicated by a long-dashed line.

CONCLUDING REMARKS

Compressor-blade cascade data have been presented in the form of design carpet plots, which greatly facilitate the selection of compressor blade sections required to fulfill velocity diagrams. Plots of this type also are shown to increase greatly the usefulness of available cascade data by providing a simple method of obtaining the off-design variation in turning angle with angle of attack.

Langley Aeronautical Laboratory,
National Advisory Committee for Aeronautics,
Langley Field, Va., August 13, 1954.

APPENDIX

CONSTRUCTION OF CARPET PLOTS

Examine first figure 3(a). It will be noted that this figure is composed of five similar and separate plots. Each of these plots shows the variation of the turning angle θ with the angle of attack α and the inlet-air angle β_1 for a given solidity σ and a camber C_{l_0} of 0.40. It might be here pointed out that the tests in reference 1 were made at four inlet-air angles, 30° , 45° , 60° and 70° . The leftmost plot, which represents a solidity of 1.50, is constructed by plotting turning angle as ordinate against angle of attack as abscissa for β_1 equal to 30° . Then, for a β_1 of 45° , the α scale is shifted to the right a number of grid units proportional to the 15° increment in β_1 and the turning angles are plotted as before. This procedure of shifting the α scale is followed until the range of β_1 's for which test data are available has been completed. Curves of constant angle of attack may then be drawn between the several curves of α against θ , so that the removal of the α abscissa scales is possible. At this point, curves of α against θ may be filled in at 5° intervals of β_1 by using the proper abscissa increment. The plot thus constructed is called a θ, α, β_1 carpet.

A θ, α, β_1 carpet is constructed for the next solidity of 1.25 by shifting the angle-of-attack scales to the right a number of grid units proportional to the solidity increment of 0.25 and sufficient to keep any overlapping of the θ, α, β_1 carpets to a minimum. This procedure previously described in constructing the first θ, α, β_1 carpet is then repeated. The full range of solidities for which test data are available (0.5 - 1.5) may be presented by spacing and constructing the θ, α, β_1 carpets on this plot called a $\theta, \alpha, \beta_1, \sigma$ carpet plot. Similar $\theta, \alpha, \beta, \sigma$ carpet plots are then made for each of the other cambers, 0.8, 1.2, 1.5, and 1.8 shown by figures 3(b), 3(c), 3(d), and 3(e), respectively.

For intermediate camber conditions, linear interpolations between $\theta, \alpha, \beta_1, \sigma$ carpets could be used or these $\theta, \alpha, \beta_1, \sigma$ plots could be combined into a single carpet plot to make possible a single graphical interpolation. For example, figure 3(a) may be combined with figure 3(b) by again shifting the angle-of-attack scales to the right a number of grid units proportional to the camber increment of 0.40. To avoid overlapping of the $\theta, \alpha, \beta_1, \sigma$ carpets, the θ ordinate scale can also be shifted vertically a number of grid units proportional to the camber increment of 0.40. This combination of a vertical and a horizontal shift is facilitated by the use of register points marked "AB" on both plots 3(a) and 3(b). The AB register points can be superimposed and the

grids aligned. In like manner, using all of the register points, figures 3(a), 3(b), 3(c), 3(d), and 3(e) may be assembled into a single carpet plot. Figure 3(f) was made by combining plots 3(a), 3(c), and 3(e) representing cambers of 0.4, 1.2, and 1.8, respectively. On this carpet, the design angle of attack is indicated by a dotted line and the approximate occurrence of twice minimum drag is indicated by a dashed line. Since the origins of the θ scales for cambers of 1.2 and 1.8 are shifted vertically a number of grid units proportional to the camber increment, the ordinate scale is no longer a true θ scale for these higher cambers and is called R. When an interpolation is made for any camber above 0.4, the θ value may be obtained by substituting R in the following expression:

$$\theta = R - 50(C_{l_0} - 0.4)$$

A larger (32 inch by 54 inch) copy of figure 3(f) may be obtained from NACA Headquarters, Washington, D. C. Figures 3(b) and 3(d) representing cambers of 0.8 and 1.5 were omitted from this plot in order to reduce the size of the plot. It will also be noted that data are available for cambers of 0.8 and 1.5 at only two solidities, 1.0 and 1.5.

REFERENCES

1. Herrig, L. Joseph, Emery, James C., and Erwin, John R.: Systematic Two-Dimensional Cascade Tests of NACA 65-Series Compressor Blades at Low Speeds. NACA TN 3916, 1957. (Supersedes NACA RM L51G31.)
2. Yates, A. H.: 'Carpets' and 'Lattices'. Aircraft Engineering, vol. XVIII, no. 203, Jan. 1946, pp. 8-9.
3. Erwin, John R., and Yacobi, Laura A.: Method of Estimating the Incompressible-Flow Pressure Distribution of Compressor Blade Sections at Design Angle of Attack. NACA RM L53F17, 1953.

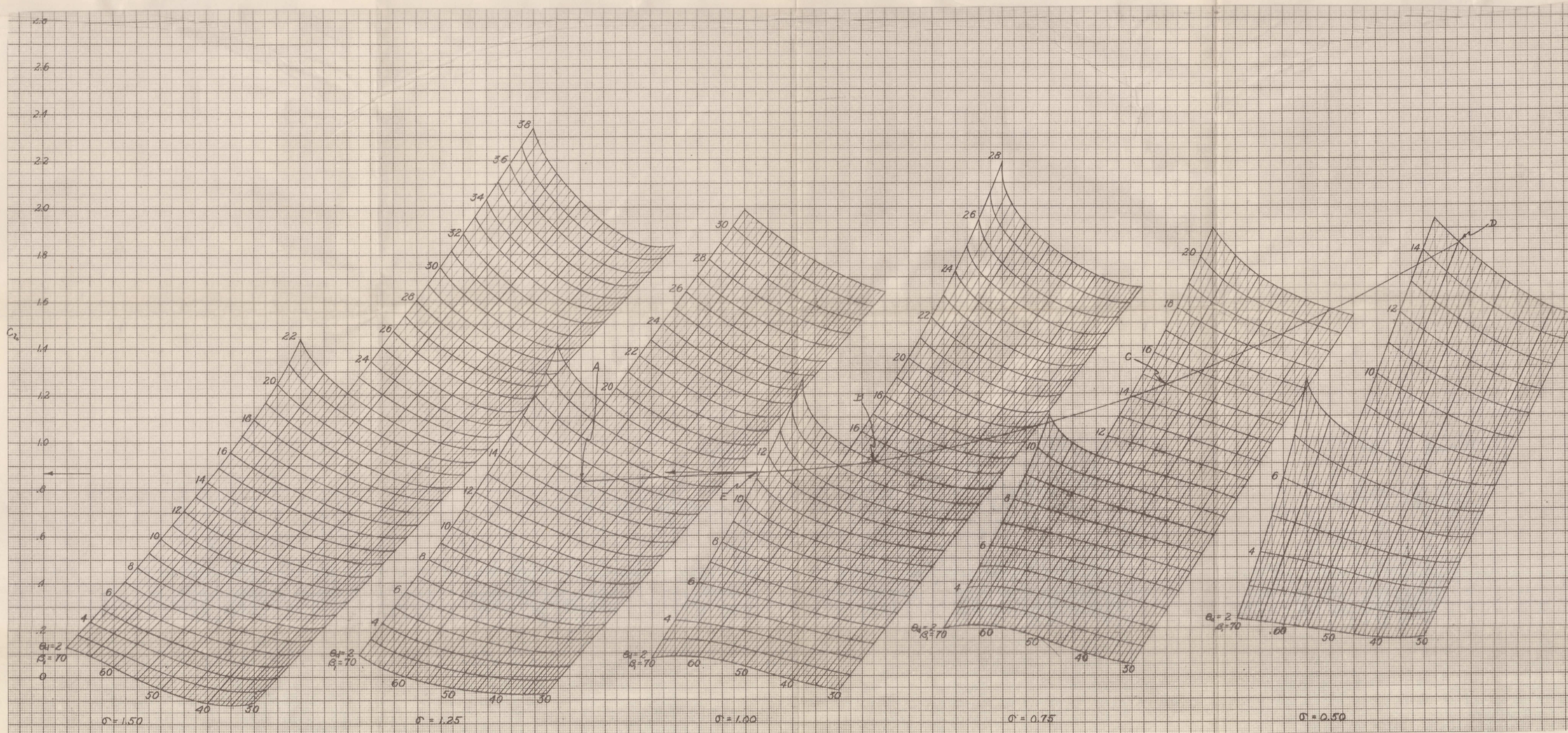
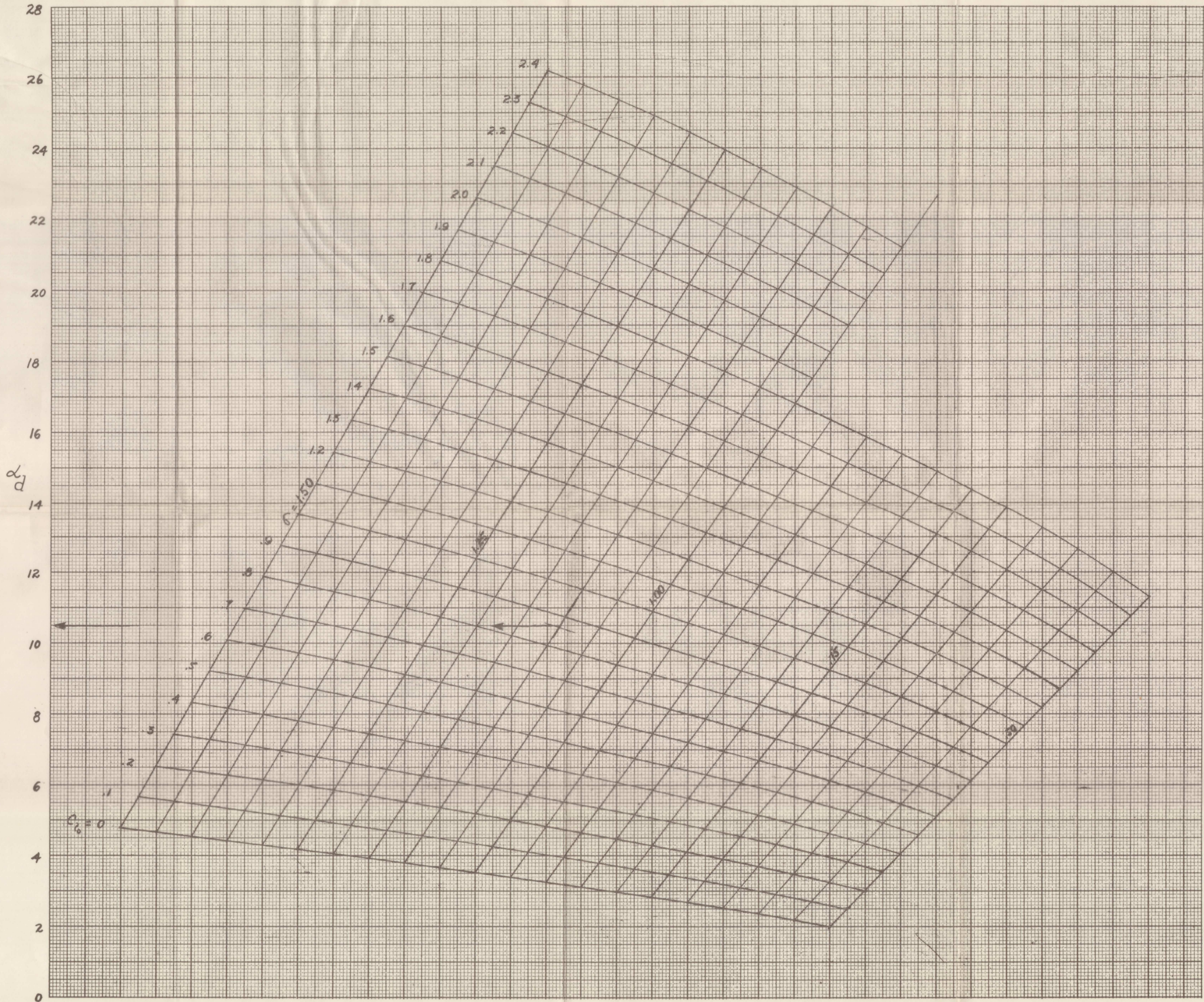
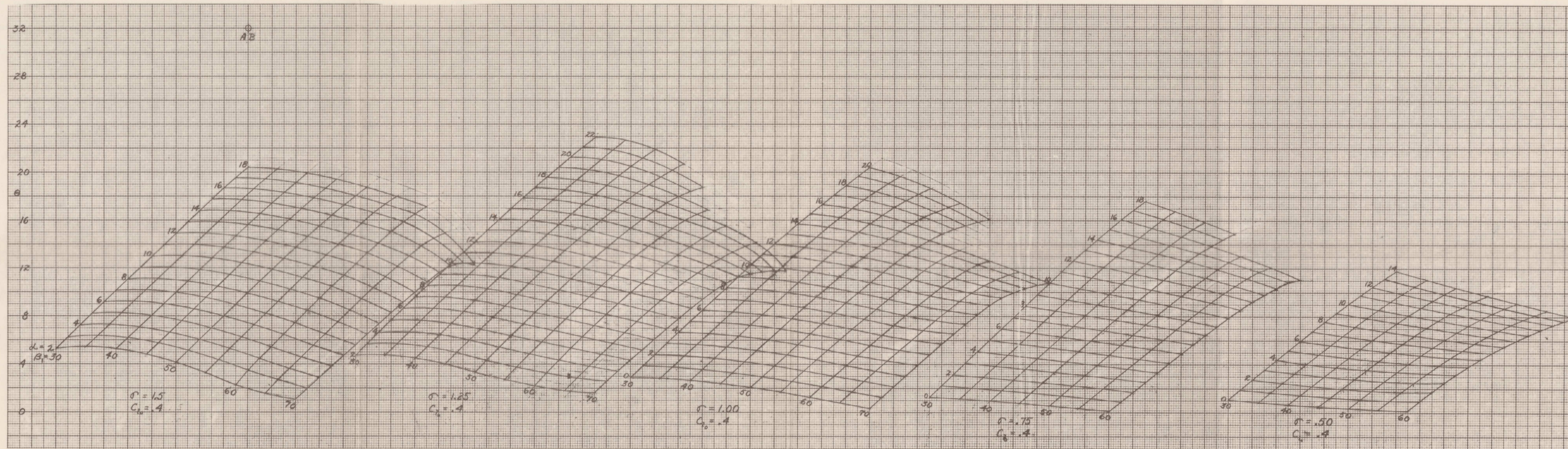


Figure 1.- Design-camber selection chart for NACA 65-(Cl₀A₁₀)₁₀ sections.

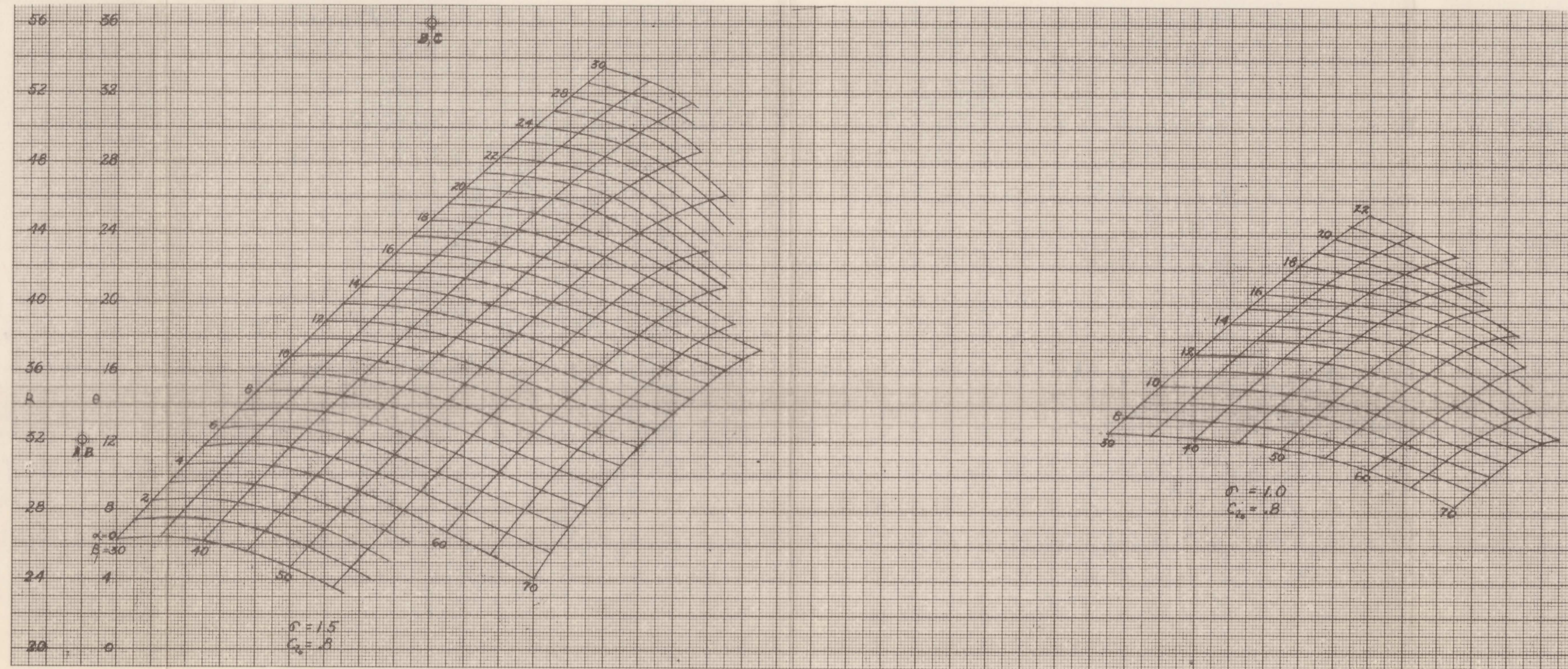


3117 SEP



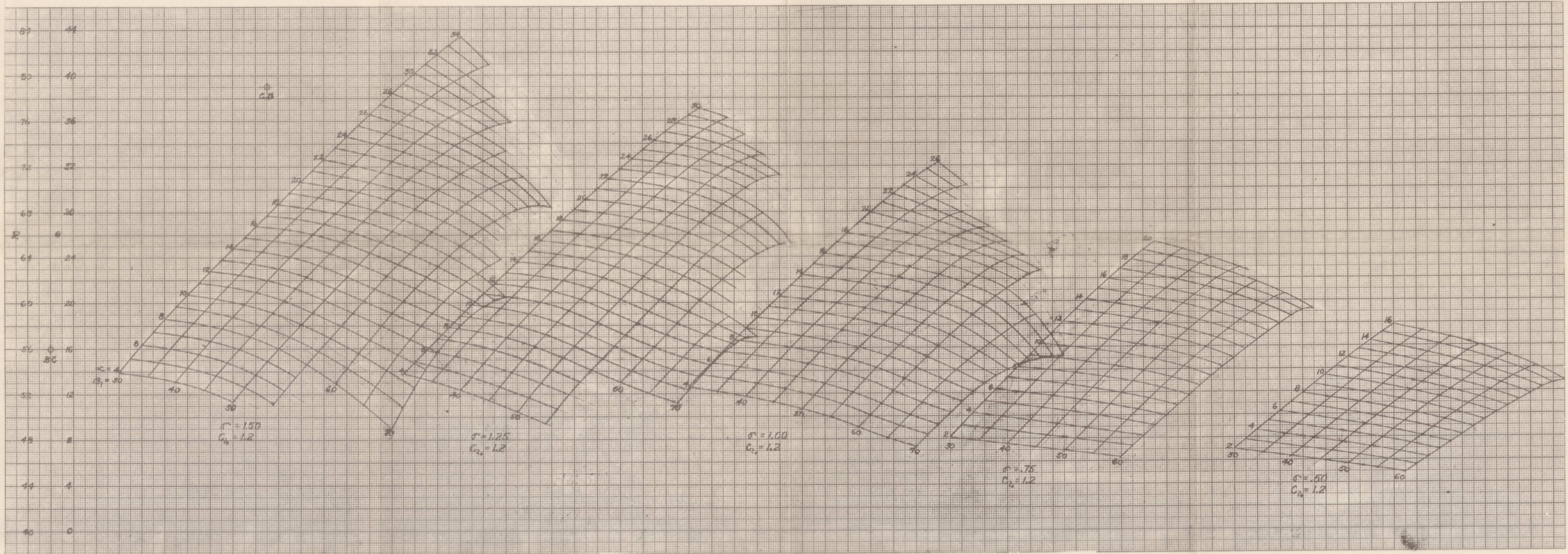
(a) NACA 65-(4A10)10 section; $C_{L_0} = 0.4$.

Figure 3.- Off-design turning-angle carpets for NACA 65-series compressor blades.



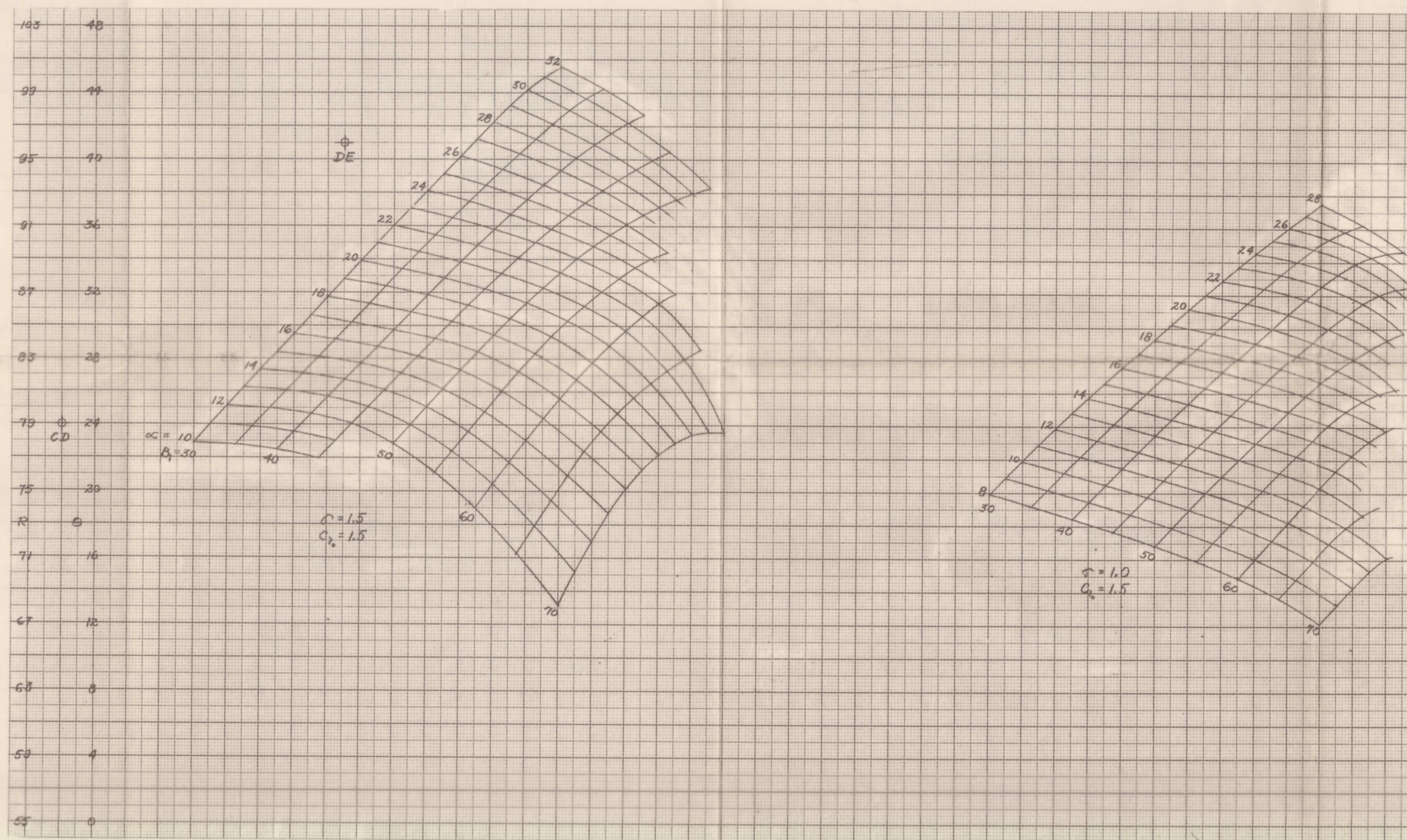
(b) NACA 65-(8A₁₀)10 section; $C_{l_0} = 0.8$.

Figure 3.- Continued.



(c) NACA 65-(12A₁₀)10 section; $C_{l_0} = 1.2$.

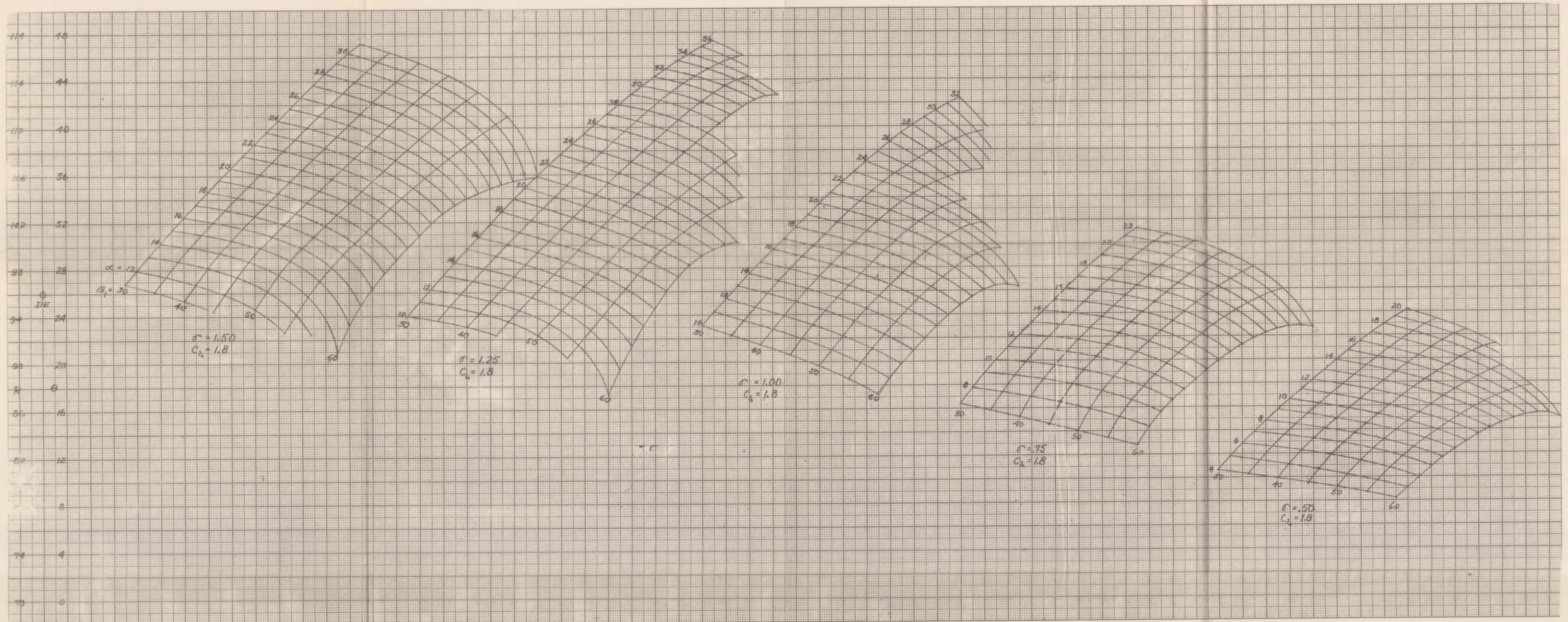
Figure 3.- Continued.



(d) NACA 65-(15A₁₀)10 section; $C_{l_0} = 1.5$.

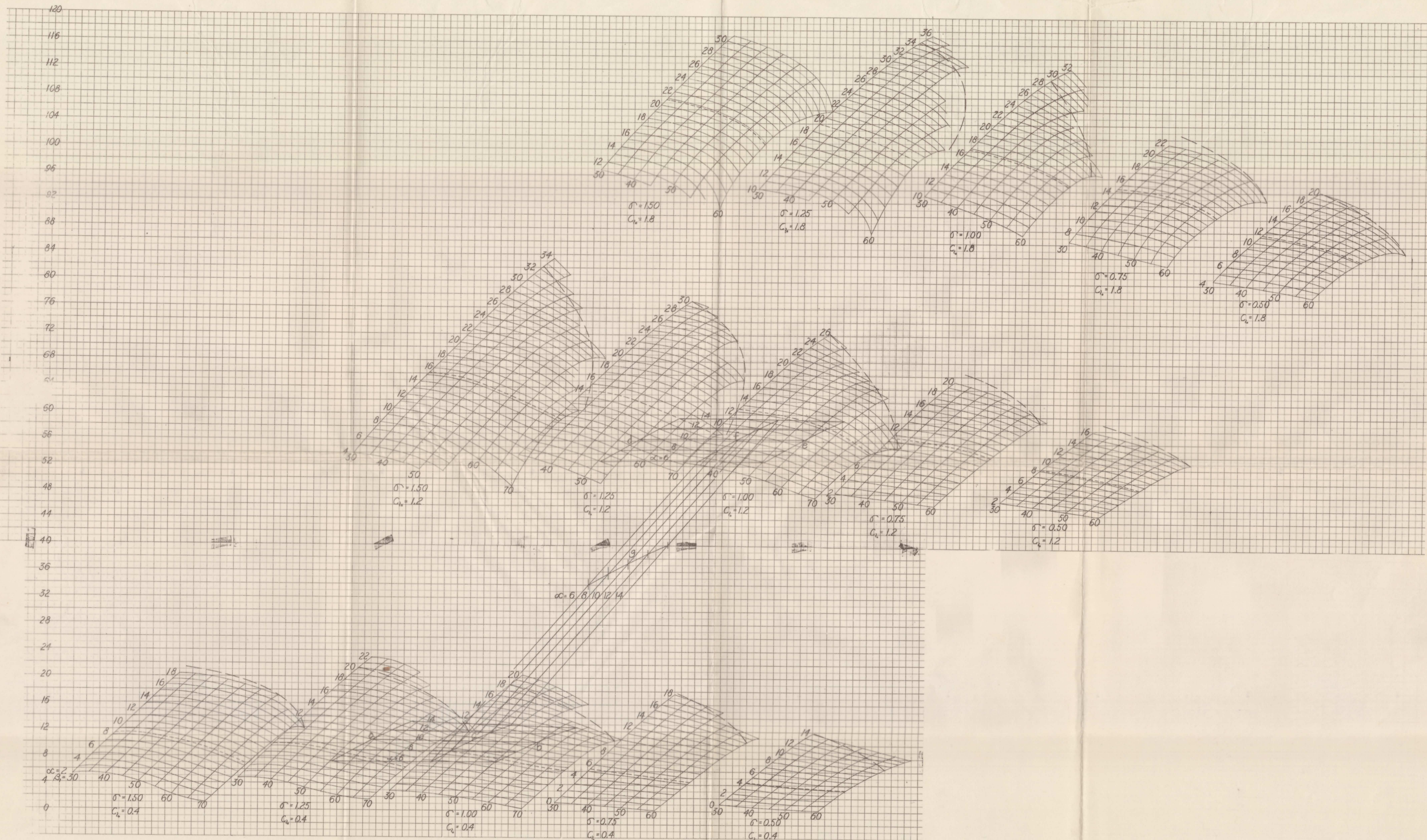
Figure 3.- Continued.

8381115



(e) NACA 65-(18A₁₀)10 section; $C_{L_0} = 1.8$.

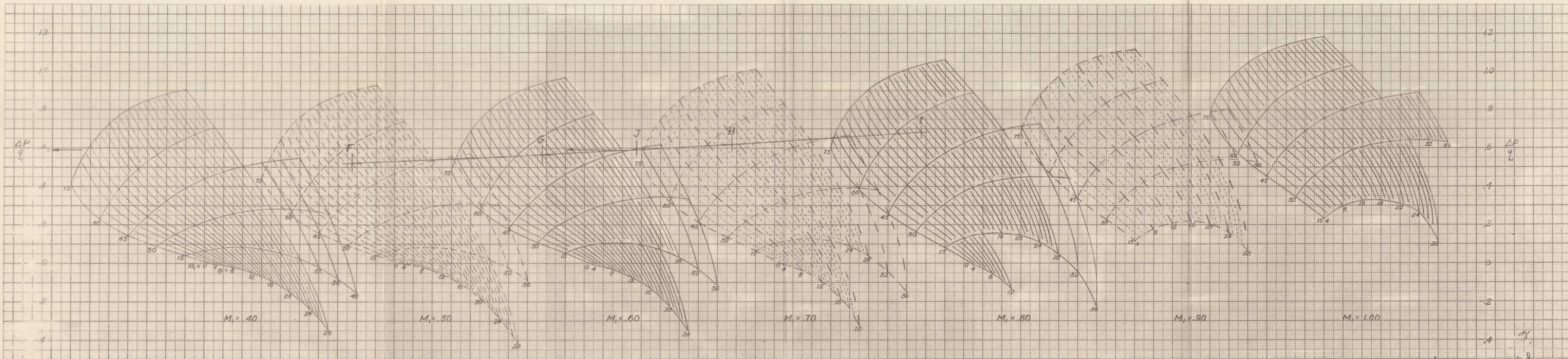
Figure 3.- Continued.



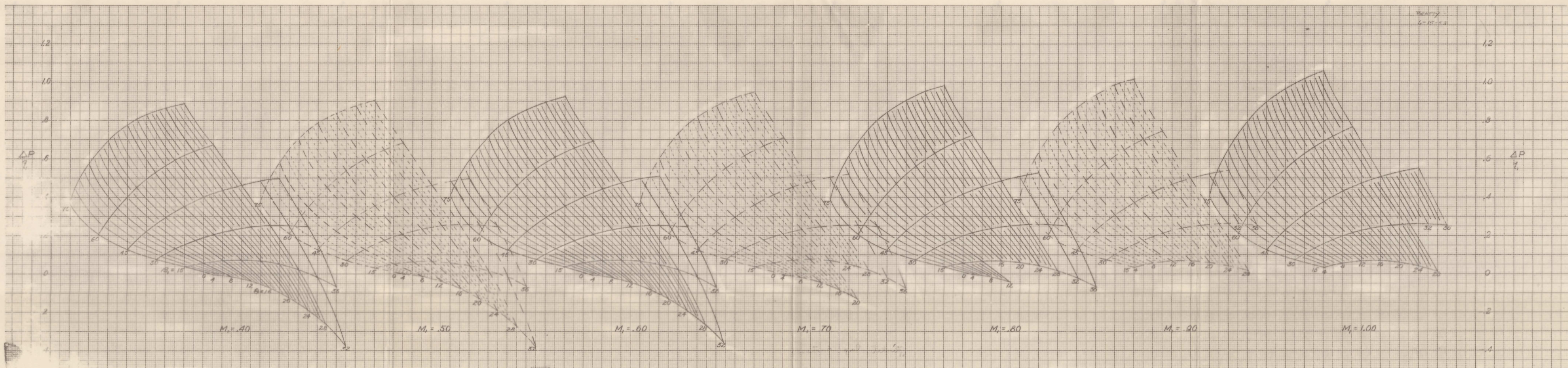
(f) Composite of off-design carpets for NACA 65-series sections for values of C_{l_0} of 0.4, 1.2, and 1.8.

Figure 3.- Concluded.

8114 SEP



(a) Constant stream-tube area.



(b) Constant axial velocity.

Figure 4.- Pressure-rise-coefficient carpets.